

MANUFACTURING HYBRID LIGHTWEIGHT COMPOUNDS OF CLOSED-CELL ALUMINIUM FOAM AND THERMOFTENING PLASTICS IN INJECTION MOULDING PROCESSES

*Steffen, M. E.
Koch, M.*

Technische Universität Ilmenau, Fachgebiet Kunststofftechnik

ABSTRACT

Towards the background of rising energy cost and the shortage of resources, lightweight materials become more important in industrial and automotive applications. Nowadays, vehicle designers try to reduce the weight by substituting high-density materials with low-density compounds of similar mechanical properties. This work deals with the development of a new hybrid-material combination consisting of aluminum foam and thermoplastic. As a result of the porous cell structure, aluminum foams show a low weight with a comparatively high stiffness. In combination with a thermoplastic material the distinctive features of both materials can be combined to obtain a new composite material, which unifies their remarkable characteristics. After primary co-processing, strength and stiffness characteristics of such structural components have not been tested yet and will be examined.

Index Terms – Aluminum foam, hybrid lightweight material, injection molding

1. INTRODUCTION

Additionally to a pure weight reduction the demand for enhanced mechanical properties, such as stiffness and strength, grows in lightweight design. New hybrid lightweight materials consisting of closed-cell Aluminum foam and thermoplastics represent a promising approach, whose potentials are widely unknown. The enclosed gas volume and the associated high porosity of foams are leading to low densities and thus low component weights are achievable. The metallic base material provides high mechanical strength, making metal foams ideal for lightweight applications. Based on previous works, it can be assumed that a foam core surrounding plastic layer may increase the mechanical properties. The enclosing plastic layer can also be used to integrate fasteners and provides an enhanced load transmission into the foam. [HLP07, AEF00, GiA97]

To successfully produce such hybrid materials in the injection molding process it is necessary to describe and detail the essential process parameters. Mold filling in injection molding processes is theoretically well understood, but only transferable to reality as the corresponding simplifications for the boundary conditions are appropriate. The undefined surface conditions of the aluminum foam do not fulfill this requirement. Unsteady transitions, nonisothermal conditions, and not fully known rheological behavior of the floating interface between the inhomogeneous foam surface and the plastic melt causes an additional complexity.

The low pressure resistance of the aluminum foam is contrary to the upcoming high pressures in injection molding processes. High pressures causing the outer surface cells to break and an injection of the foam structure by plastic melt occurs. This paper deals with the development

of a model, which describes the interrelation between the foam density and its pressure resistance.

The remarkable influences for manufacturing the hybrid-compound have been identified in this study. First of all, the pressure resistance of the foam has theoretically been examined by describing the irregular surface properties with simplified geometric bodies and their statistical distribution. Based on this, a model has been created which depicts the pressure resistance analytically. To verify the model, an injection molding tool has been designed and manufactured which allows the foam cores to overmold under varying conditions. Injection pressures and the dimensions of the core have been modified to define the amount of plastic-injected cells.

The properties of the foam strongly depend on its mixture ingredients, its manufacturing route and pores characteristics, which will be discussed later in this paper. Metal Foams are solid metal materials, commonly aluminum, with a large volume of gas-filled pores. The Pores are present in an open- or closed-cell structure. Open cell structures are characterized by reticulated structures that have no distinct cell walls. Closed-cell foams in contrast, having vesicular structures with distinct cell walls. The two cell structure types are shown in the following Figure 1. [HLP07, GiA97]

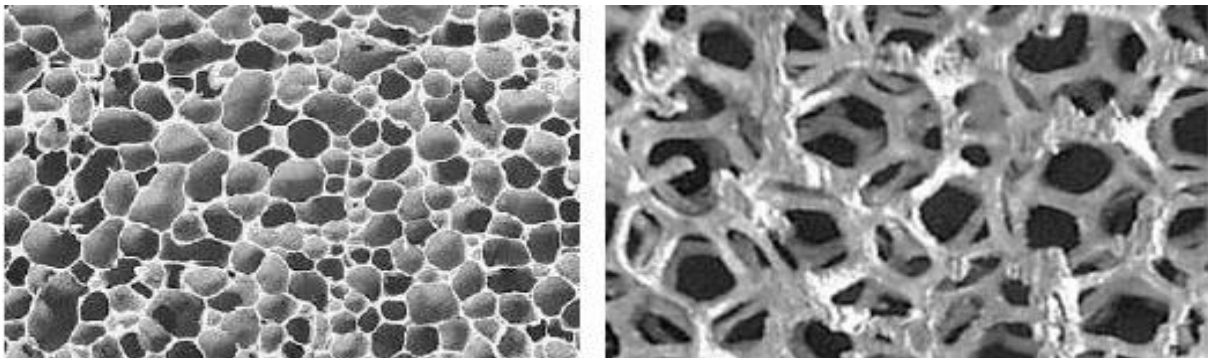


Figure 1: closed-cell (left) and opened-cell (right) foam structures [Lan13]

An injection molding processes is used to overmold the foam cores. It is one of the most common manufacturing processes for thermoplastic parts. In thermoplastic injection molding processes synthetic granules is fed into the machine. An injection unit mixes and melts the material. If enough material is melted up, the injection phase begins. The screw acts like a ram and forces the melt into a temperature controlled mold via a channel system of gates and runners.

2. METHOD

2.1 Materials

Polypropylene (PP) and closed-cell aluminum foams of different densities and production methods are used in this study. The polypropylene type INEOS 400-CA70 possesses a melt-flow-rate (MFR) of 70 g/10 min at 240 °C and 2.16 kg. This plastic was chosen because of its low viscosity that leads to decreasing injection pressures.

For closed-cell foams, powder- and melting metallurgical production processes have been prevailed. In both processing methods metal powder and a blowing agent, typically titanium hydride, are needed. In some cases, other substances are added to stabilize the process.

In manufacturing processes based on powder metallurgical variants, metal powder and blowing agent are mixed together and being compacted by hot isostatic pressing or bar extrusion techniques. The fabricated bar shaped product can be foamed in a subsequent step. Therefore, the semi-finished products have to be heated above the melting point of the metal component, whereby the titanium hydride releases hydrogen gas which causes the mixture to foam. [AEF00, GiA97]

In the melt metallurgical variant, the metal exists in a molten state. By adding additional solid components, often 1-2% calcium, the viscosity of the melt is increased. Under constant stirring operation titanium hydride is added, which splits to titanium and gaseous hydrogen and provides the formation of foam. [AEF00]

For the examinations melt and powder metallurgical produced foams were used. The melt metallurgical foams have a density of 0.3 g / cm^3 . The used powder metallurgical foams have densities of 0.6 g / cm^3 and 1.0 g / cm^3 . Different densities provide the possibility to make statements about the density depending properties. Due to the uneven pore distribution density changes of up to 20% can be reported. In order to preserve the clarity, the samples are classified in one of stated density classes.

2.2 Characterization of the foam surface

For the development of a model which describes the pressure resistance, the knowledge of the surface is an essential. The penetration of plastic is because the relatively thin cell walls break down under high pressure. This approach aims to express the parameters of pore wall thickness and cell-sizes as a function of the density. These parameters can be derived by using image processing techniques. Starting point for the determination of cell wall thickness and pore radius are cross-section samples of three different aluminum foams.

The specimens were first cut, dyed black and polished. Due to the strong contrast between the black colored pores and the metallic-silver colored cell walls the separation is easy. The cross-sectional area of the samples is 70 mm wide and 20 mm high.

In a first step, an image of the cross-section is binarized. As described in the following formula, the ratio of the true cross sectional area A_{CS} and its number of pixels n_{global} can be determined by the formation of a quotient Q .

$$Q = \frac{n_{global}}{A_{CS}} \left[\frac{\text{Pixel}}{\text{mm}^2} \right] \quad (1)$$

To characterize the pores of the sample, the black-dyed pores can be manually superimposed with circular elements. With the help of Q , the number of pixels of the superimposed circular areas can be converted into true values. With that, the radius of the pore r_{pore} can be calculated by changing the area equation of a circle A_{pore} with respect of Q and the number of pixel.

$$A_{pore} = \pi \cdot r_{pore}^2 \quad \rightarrow \quad r_{pore} = \sqrt{\frac{A_{pore}}{\pi}} \quad \text{with} \quad A_{pore} = \frac{n_{circle}}{Q} \quad (2)$$

The number of pores is density dependent. About 800 pores could be detected on a density of 1.0 g/cm^3 and 250 pores at a density of 0.3 g/cm^3 . This arises from a smaller pore size with increasing density and the associated, higher aluminum content in the material. In the following Figure 2 the distributions of the pore radii are presented.

2.3 Modell to describe the pressure resistance

The approach aims to reduce the input parameters to a minimum. As the injection pressure acting on the surface of the foam, the data for the pore sizes and cell wall thicknesses determined previously are used as basis for the model. A tensile test was performed on the starting material and yield strength of about 100 MPa could be determined. For simplicity the following assumptions are made.

- There are no sink marks and breakthroughs in the material
- The material properties of the metal component are constant
- The permissible strength of the metal component is coincident with the precursor material

The model based on a simple bending. It is assumed that the cell wall is tangentially connected to two idealized pores. The distance of the bearings, and thus the length of the bending beam correspond to the pore diameter. The height corresponds to the cell wall thickness. The occurring pressure acts as area load on the bending bar. The abstracted model is shown in Figure 4.

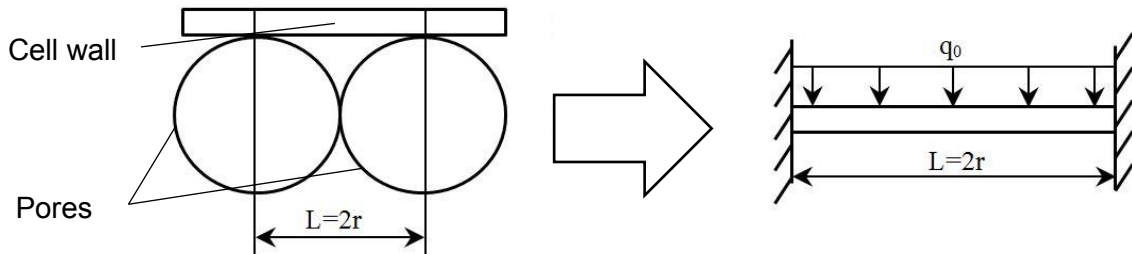


Figure 4: Abstracted model, based on a bending beam

A stress analysis for bending can be taken to calculate the model. Therefore, allowable and existing stresses can be equated. To calculate the maximum allowable pressure p_{max} on the aluminum foam, it is necessary to know the force F on the respective surface A_{Beam} . The following approach is a calculation of this value, based on the bending moment M_b , the section modulus W_b , and height h and length l of the beam. The allowable stress can be replaced by the yield strength.

$$p_{max} = \frac{F}{A_{Beam}} ; M_b = \frac{F \cdot l}{12} ; \sigma_{alo} = \frac{M_b}{W_b} ; W_b = \frac{l \cdot h^2}{6}$$

$$p_{max} = \frac{2 \sigma_{alo} h^2}{l^2} \quad (3)$$

By decomposing the bending moment and section modulus of the equation, the input parameters can be reduced on the bending beam length, bending beam height and yield strength. Bending beam length and bending beam height can be substituted by cell wall thickness and pore radius. The pressure resistance is now a function of cell wall thickness, pore radius and yield strength.

$$p_{max} = f(l, h, R_e) \rightarrow f(r, s, R_e)$$

Substituting the data from the previous experiments, there are density-dependent areas. This is graphically shown in Figure 5.

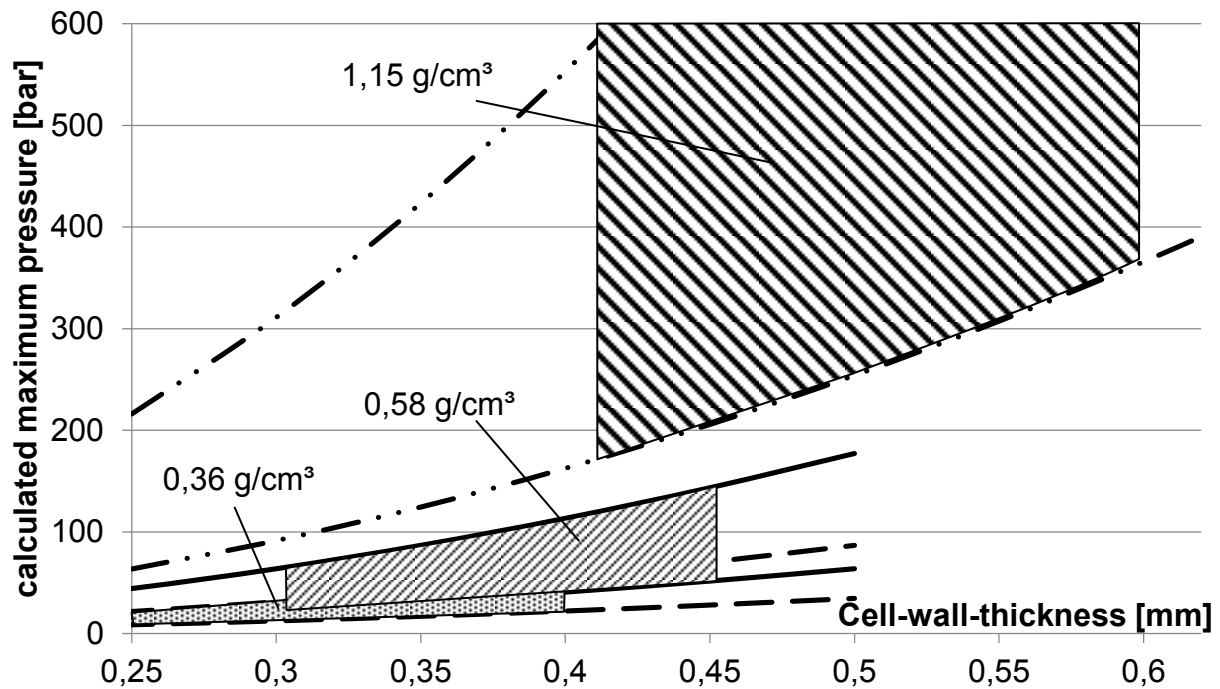


Figure 5: Density related pressure resistance areas[LiS14]

The designated areas in the figure are fields which describes the maximum theoretically pressures. Thinner cell-walls and larger pore sizes tend to break at lower pressures, thicker walls and smaller pores at higher pressures. The vertical limits result from the identified cell wall thicknesses, the horizontal boundaries are derived from the respective pore radii. Smaller pores radii can be found in the upper part of the fields, larger radii at the bottom. For the cell wall thicknesses it is the same. In right pane of the respective field, thicker cell walls can be found, leaner in the left pane. Thus, the distribution of the pores in the model is taken into account.

2.4 Molding Tool

In order to verify the theoretical model, an injection molding tool was designed and fabricated. Prepared specimens were coated with the PP on one side (Figure 6).

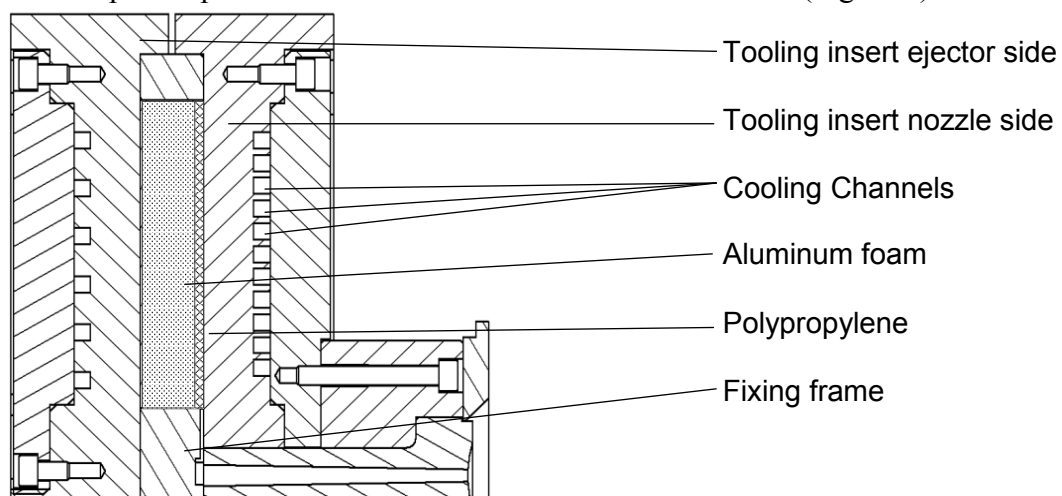


Figure 6: Molding tool

3. RESULTS

An injection molding machine type FM 60 was used to produce the one-sided hybrid compounds. A constant melt temperature of 240 °C, a mold temperature of 80 °C and a screw speed of 0.01 m/s were used for the experiments. The density and thicknesses of the plastic-layer have been varied. On the images of the cut hybrid-compound, the difference between a filled and non-filled compound can be seen.

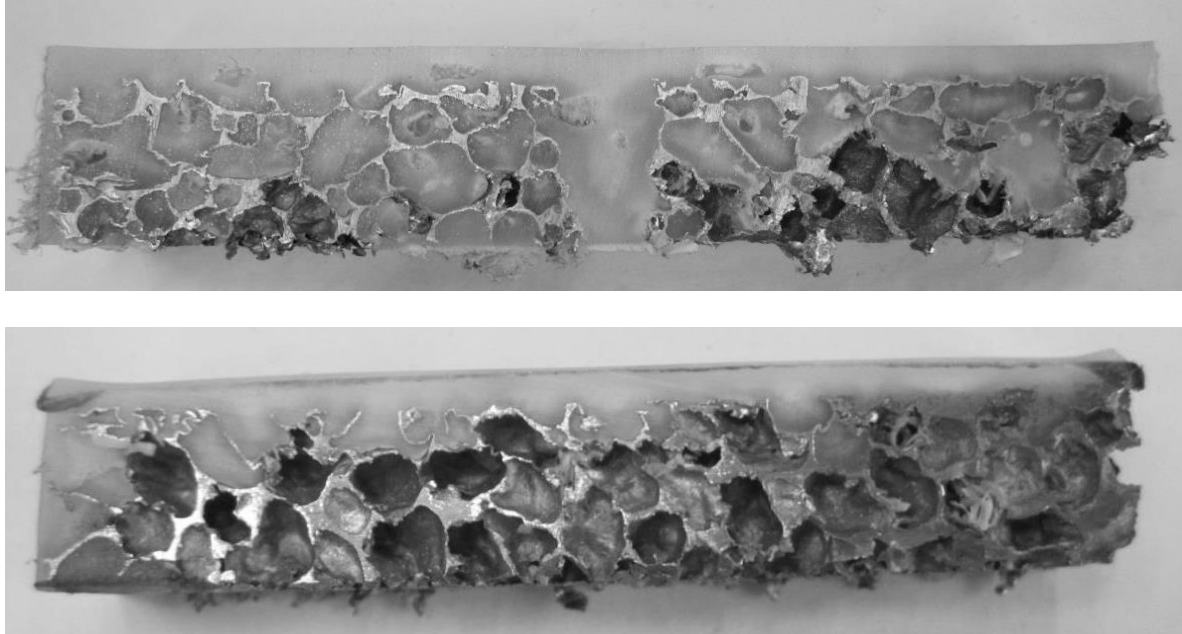


Figure 7: filled and unfilled compound

The following figure depicts the penetrated pore volume over the injection pressure. As expected, a higher injection pressures leads to an increased penetration of the pores. With increasing densities, this effect is getting smaller.

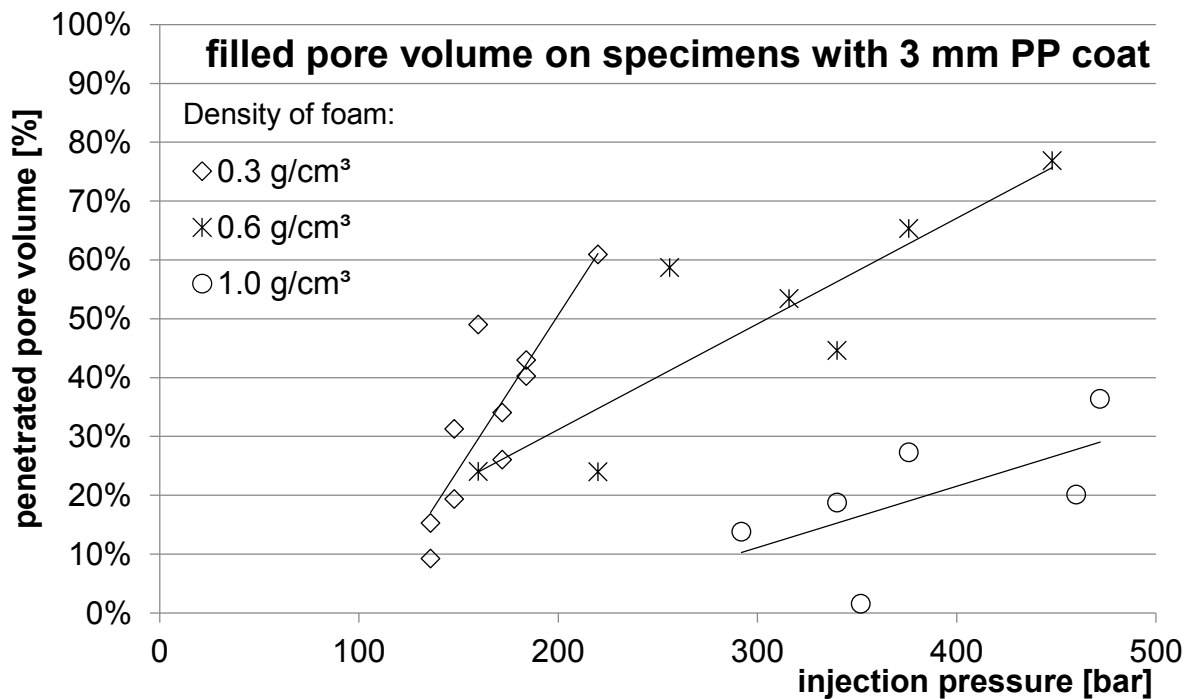


Figure 8: filled pore volume on different densities

4. DISCUSSION

The studies have shown a way to produce hybrid compound. The previous results have shown that dependence between the foam density and its pressure resistance exists. Initial statements about the amount of process pressures could be derived and the necessary geometric values of the foam have been characterized successfully. The accuracy of the created theoretical models is presently being investigated. Additionally, arrangements for the manufacturing of three-dimensional components are in preparation to strengthen the preliminary findings.

REFERENCES

- [HLP07] T. Hipke, G. Lange, R. Poss, Taschenbuch für Aluminiumschäume, Aluminiumverlag, Düsseldorf, 2007
- [AEF00] F. Ashby, A. Evans, A. Fleck; Metal Foams a Design Guide, Butterworth-Heinemann, Woburn, 2000
- [GiA97] L. J. Gibson, M. F. Ashby, Cellular solids structure and properties, Cambridge University Press, Cambridge, 1997
- [Bau95] J. Baumeister, J. Banhart, M. Weber, VDI Berichte 1235-Neue Werkstoffe im Automobilbau-Hocheffiziente Energieabsorber aus Aluminiumschaum, VDI-Verlag, Bremen, 1995
- [LiS14] M. Lindhof, J. Sinn, Herstellung und Charakterisierung eines spritzgegossenem Kunststoff-Metallschaum Verbundes für automobile Anwendungen, Student-project, TU Ilmenau, 2014

CONTACTS

M. Sc. Maik Eno Steffen
Prof. Dr.-Ing. Michael Koch

maik-eno.steffen@tu-ilmenau.de
michael.koch@tu-ilmenau.de